2021 43rd Annual International Conference of the
IEEE Engineering in Medicine & Biology Society (EMBC)
Oct 31 - Nov 4, 2021. Virtual Conference

Mechanical Analysis of the Quadruple Butterfly Coil during Transcranial Magnetic Stimulation and Magnetic Resonance Imaging*

Oluwaponmile F. Afuwape, Winnie M. Kiarie, Sarah A. Bentil, and David C. Jiles, *Life Fellow*, IEEE

Abstract— **Transcranial Magnetic Stimulation (TMS) is a tool for the treatment of psychiatric and neurological disorders. It involves using a transient magnetic field generated from electromagnetic coils in inducing an electric field (E-field) within the neurons of the brain. The induced E-field results in an increase in the brain membrane's electric potential, leading to polarization or depolarization of the neurons depending on the mode of treatment. There has been much development in TMS technology recently, with most research focusing on improving the performance of TMS coils at greater depths and achieving more localized stimulation. Another development has been the combination of TMS with other medical techniques such as Functional Magnetic Resonance Imaging (fMRI) and Electroencephalography (EEG) to enable accurate mapping of the brain's electrical activity during TMS. However, the TMS coils experience large forces in this new highly energized external magnetic field environment. Accurately determining the magnitude and location of the Lorentz force, torque, and stresses that the TMS coils experience in this environment becomes of utmost importance. In this chapter, the authors used finite element analysis to determine the magnitude and location of the Lorentz forces and stresses experienced by a novel TMS coil, Quadruple Butterfly Coil (QBC), in a TMS-fMRI operation. With the TMS-fMRI operation, the maximum values of the magnetic flux density, Lorentz force density, and von Mises stress were observed in the z-axis of the QBC orientation. They resulted in a 39.65 %, 38.94 %, and 94.59 % increase, respectively, from the typical TMS operation.**

Clinical Relevance— **This study is to understand the behavior of the QBC during concurrent TMS-fMRI so as to design for the mechanical stability of the QBC.**

I. Introduction

Transcranial Magnetic Stimulation (TMS) is a non-invasive technique of modulating the neurons of the brain that functions on the principle of electromagnetic induction [1]. TMS, which has been employed in research and clinically, has proven to be a useful tool for the treatment for certain neurological and psychiatric disorders such as migraine headaches, obsessive-compulsive disorder (OCD) and major depressive disorder (MDD). TMS has also been used as a tool for cognitive neuroscience [2] and also for mapping of the functional and structural connectivity of the brain.

During TMS, strong pulses of current flowing through stimulating coils positioned over the scalp of the human head generate transient magnetic fields. The generated magnetic field in turn induces electric field that alters the functioning of the brain and causes change in the plasticity of the brain's neurons [2]. This alteration results in an excitation or inhibition of the motor cortex by producing a motor evoked potential (MEP) that leads to the polarization or depolarization of the membranes of the brain at the target area [3]. The activation of the brain neurons from TMS depends on the magnitude and direction of the electric field (E-field) from the time-varying magnetic field [4]. For clinical applications, TMS are administered repetitively based on approved protocol and this means that TMS depends on the frequency of stimulation [4].

The magnitude and direction of the induced E-field from TMS is dependent on several factors including coil geometry, positioning and orientation amongst others. With coil geometry, various designs have been proposed by researchers [5]. The focality and depth of penetration of the E-field are the characteristics of the induced E-field that are of utmost importance with the different coil designs. The circular coil and the figure-of eight (FOE) coil are some of the conventional and commercially available coils for TMS [6] and are considered superficial coils. The Hesed coil, Halo coil and Triple Halo coils are coils designed for penetration of the induced E-field at greater depth, however, they exhibit reduced focality [7], [8]. The Quadruple Butterfly Coil (QBC) is a new patented coil design for a higher focality than the conventional FOE coil [9]. Coil positioning with respect to the brain tissues and anatomy also influences the effect of TMS as positioning of TMS coils at different stimulation sites results in varying modulating effects. The vertex and the dorsolateral prefrontal cortex (DLPFC) are the major neuroanatomical location considered for treatment with TMS [10]. Coil orientation can also influence the response of the brain neurons to TMS as alignment of the direction of the induced E-field and the tissue results in maximum stimulation [11].

With advancement in neuroscience studies and research, TMS has also been used in combination with other medical techniques like Functional Magnetic Resonance Imaging (fMRI) [12], and Electroencephalography (EEG) [13] to enable accurate mapping and measurement of the electrical activity of the brain during TMS. Concurrent TMS-fMRI has been used to study the response of the motor cortex to induced E-field from TMS [14], as the response of the structural and functional anatomy is visualized, hence helping to predict TMS effectiveness in treatment. However, with these combinations, new challenges arise as TMS coils are placed in a new environment. For instance, one challenge of TMS-fMRI

*This research is funded by the Barbara and James Palmer Foundation and the Stanley Chair in Interdisciplinary Engineering at Iowa State University.

O. F. Afuwape (corresponding author) is with the Departments of Mechanical Engineering and Electrical and Computer Engineering, Iowa State University, Ames, IA 50011, USA (phone: 515-817-3245; e-mail: oafuwape@iastate.edu).

W.M. Kiarie is with the Department of Material Science and Engineering, Iowa State University, Ames, IA 50011, USA (e-mail: wmkiarie@iastate.edu).

S.A. Bentil is with the Department of Mechanical Engineering, Iowa State University, Ames, IA 50011, USA (e-mail: sbentil@iastate.edu).

D.C. Jiles is with the Departments of Electrical and Computer, and Material Science and Engineering, Iowa State University, Ames, IA 50011, USA (e-mail: dcjiles@iastate.edu).

is the potential of current leaking into the TMS coil as a result of increased magnetic field from the fMRI scanner [14]. The application of shields (active or passive) to coil designs have also been confirmed to induce additional forces which results in mechanical stress on the TMS coil [15]. Accurately determining the magnitude and location of the Lorentz force and stresses that the TMS coils experience as a result of increased magnetic field becomes of utmost importance, especially when TMS coils are designed, as there might be the need for mechanical dampers or other mechanical systems to be incorporated in the design [15]. Additionally, assessing the safety of TMS when administered to patients during concurrent TMS-fMRI is necessary.

The forces experienced by the FOE coil in a typical TMS operation and in a highly external energized environment has been studied by [16]. However, in this paper, we study the response of the novel QBC in an externally applied field of 3T which is the typical field in a fMRI scanner. This study would help in the design for mechanical stability of the QBC and to assess the safety of concurrent TMS/fMRI to patients.

II. Method

A. Finite Element Analysis Model

The QBC consists of two large coils and two small coils. The large coils have the same dimension as the FOE coil and the small coils are 40 % of the large coils' dimension [9]. The two sets of coils have the same number of windings (13 for each set) and are inclined at 90° to each other. Fig. 1 shows the QBC with the large and small set of coils.

Fig. 1: The QBC showing the two sets of coils: large set (blue) and small set (red) [10].

For treatment with TMS, the electromagnetic coils are operated at an operational frequency of 2.5 kHz and supplied with a current of amplitude 5000A. The output from this simulation is comparable to a conventional TMS stimulator used in clinical applications [1]. In this work, we perform computational finite element analysis using COMSOL Multiphysics to simulate the TMS parameters and the applied external magnetic field.

B. Equations

The finite element modeling approach used in this paper seeks to model the transient magnetic field generated during TMS by solving Maxwell's equations as follows,

$$\nabla \cdot \boldsymbol{B} = 0 \quad (1)$$

$$\nabla \times \boldsymbol{H} = \boldsymbol{J} \quad (2)$$

Where $\boldsymbol{B}$ is magnetic flux density, $\boldsymbol{H}$ is magnetic field, and $\boldsymbol{J}$ is current density. The magnetic behavior of a magnetic material is described using the constitutive relation,

$$\boldsymbol{B} = \mu_0(\boldsymbol{H} + \boldsymbol{M}) \quad (3)$$

Where μ_0 is the permeability of free space and $\boldsymbol{M}$ is magnetization of the material, which is the magnetic moments in a given material per unit volume. In the finite element method (FEM), which is the method used in this work, (2) and (3) are solved using the magnetic vector potential $\boldsymbol{A}$ defined by the relation:

$$\boldsymbol{B} = \nabla \times \boldsymbol{A} \quad (4)$$

The Coulomb gauge transformation is defined by $\nabla \cdot \boldsymbol{A} = 0$ while the induced current density, $\boldsymbol{J}$ is calculated from Ohm's law:

$$\boldsymbol{J} = \boldsymbol{\sigma E} + \frac{\partial \boldsymbol{D}}{\partial \boldsymbol{t}} \quad (5)$$

Where $\boldsymbol{\sigma}$ is the electric conductivity, $\boldsymbol{E}$ is the induced electric field calculated from the transient magnetic field using the quasi-static approximation of TMS, and $\boldsymbol{D}$ is the electric flux density.

$$\nabla \times \boldsymbol{E} = -\frac{\partial \boldsymbol{B}}{\partial \mathrm{t}} \quad (6)$$

The induced current density $\boldsymbol{J}$, produces a Lorentz force density given by:

$$\boldsymbol{f} = \boldsymbol{J} \times \boldsymbol{B_{total}} \quad (7)$$

Where:

$\boldsymbol{B_{total}} = \boldsymbol{B}$ (typical TMS operation)

$\boldsymbol{B_{total}} = \boldsymbol{B} + \boldsymbol{B_{fMRI}}$ (external energized environment)

The Maxwell stress tensor is used to calculate the von Mises stress and is given by:

$$T_{i,j} = \varepsilon_0 \left(E_i E_j - \frac{1}{2}\delta_{i,j}E^2\right) + \frac{1}{\mu_0}\left(B_i B_j - \frac{1}{2}\delta_{i,j}B^2\right) \quad (8)$$

$i, j = x, y, z$

Where ε_0 is the permittivity, $\delta_{i,j}$ is Kronecker Delta, and $T_{i,j}$ is the element i, j of the Maxwell Stress tensor.

Since TMS coils are made from ductile material (copper), the criterion used to assess the failure of the coil was calculated from the von Mises stress, σ_v, given by:

$$\sigma_v = \left[\begin{matrix} T_{xx}^2 + T_{yy}^2 + T_{zz}^2 - T_{xx}T_{yy} - T_{xx}T_{zz} \\ -T_{yy}T_{zz} + 3\left(T_{xy}^2 + T_{xz}^2 + T_{yz}^2\right) \end{matrix}\right]^{1/2} \quad (9)$$

III. Results And Discussion

A. Typical TMS Operation

The maximum magnetic flux density generated in the QBC during a typical TMS operation (in the absence of an externally applied magnetic field) was computed to be 5.7 T. The maximum Lorentz force density and von Mises stress were computed to be 4.34×10^9 N/m^3 and 2.59×10^7 Pa respectively. The magnetic flux density, Lorentz force density and von Mises stress distribution of the QBC generated in the typical TMS operation is presented in Fig. 2. The action of the Lorentz force was also observed to act on the inner windings of the small sets of coils. The direction in which the force act is as shown in Fig. 2b. Although, the magnitude of the von Mises stress (2.59×10^7 Pa ~ 26 MPa) is lower than the yield strength of copper (~ 70 MPa), which is the failure criterion, more consideration needs to be given to the design of the small sets of coils since the maximum stress was found to act on the inner windings of the small sets of coils.

B. External Energized Environment

a) x- axis of the QBC orientation

The behavior of the QBC under the action of an external magnetic field of 3T applied in a direction parallel to the *x*-axis of the QBC orientation was analyzed and the maximum magnetic flux density was computed as 6.54 T. The effect of

this additional field is also seen on the surface of the large set of coils, when compared to a typical TMS operation. The resultant Lorentz force density and von Mises stress were computed to be 4.96 × 10^9 N/m^3 and 3.31 × 10^7 Pa respectively. This yielded an additional 14.29 % and 27.80 % in the Lorentz force density and von Mises stress respectively. The magnetic flux density, Lorentz force density and von Mises stress distribution of the QBC generated in the external field aligned with the *x*-axis of the QBC is presented in Fig. 3. The resultant Lorentz force was observed to act in a direction dependent on the flow of current in the coil as depicted in Fig. 3b.

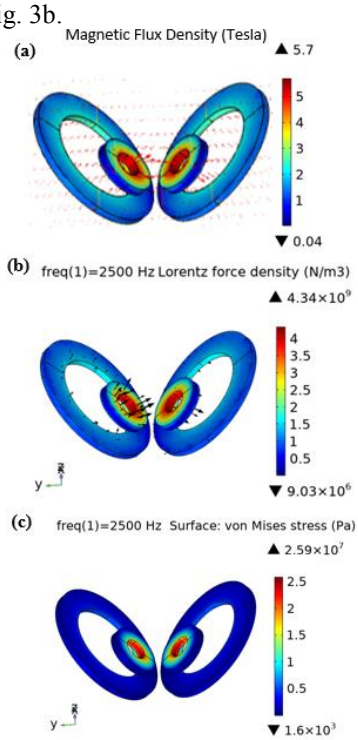

Fig. 2. (a) Magnetic flux density, $\boldsymbol{B}$ (T), (b) Resultant Lorentz force density, $\boldsymbol{f}$ (N/m^3), and (c) von Mises stress, σ_v (Pa) of the QBC in a typical TMS operation. The arrows show the direction of the magnetic field and the Lorentz force acting on the QBC for the typical TMS operation.

b) y- axis of the QBC orientation

Under the action of an external magnetic field of 3T applied in a direction parallel to the *y*-axis of the QBC orientation, the behavior of the QBC was analyzed and the maximum magnetic flux density was computed as 5 T. Resultant Lorentz force density and von Mises stress were computed to be 3.19 × 10^9 N/m^3 and 2 × 10^7 Pa respectively, yielding a 26.49 % and 22.78 % reduction in the Lorentz force density and von Mises stress respectively. In this analysis, the effect of the additional field is observed mostly on the large set of coils and the direction of the resultant forces also depends on the flow of current (see Fig. *4*b). The magnetic flux density, Lorentz force density and von Mises stress distribution of the QBC generated in the external field aligned with the *y*-direction of the QBC is presented in Fig. 4. The maximum stresses are observed to occur at the top surface of the large sets of coils.

c) z-axis of the QBC orientation

Application of the external magnetic field in a direction which aligns with the *z*-axis of the QBC yielded a magnetic

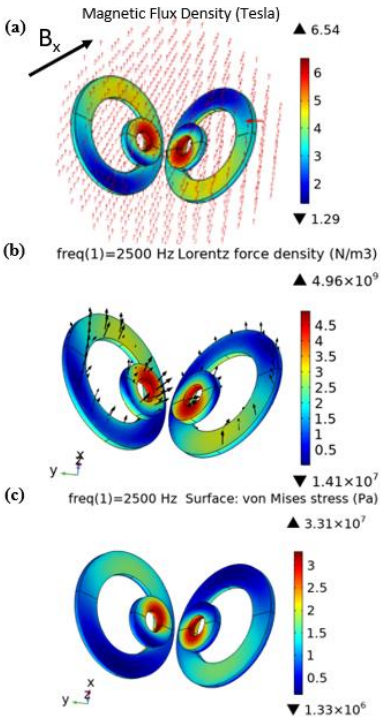

Fig. 3. (a) Magnetic flux density, $\boldsymbol{B}$ (T), (b) Resultant Lorentz force density, $\boldsymbol{f}$ (N/m^3), and (c) von Mises stress, σ_v (Pa) of the QBC in an energized magnetic environment applied parallel to the *x*-direction of the QBC. The arrows depict the external field acting on the coils in the *x*-axis direction.

flux density of 7.96 T. The additional field is observed to significantly affect the inner turn of the small right coil. The resultant Lorentz force density and von Mises stress were computed to be 6.03 × 10^9 N/m^3 and 5.04 × 10^7 Pa respectively. This resulted in about an additional 38.94 % and 94.59 % in the Lorentz force density and von Mises stress respectively. The magnetic flux density, Lorentz force density and von Mises stress distribution of the QBC generated in the external field aligned with the *z*-axis of the QBC is presented in Fig. 5. The resultant Lorentz force was observed to act dependent on the direction of the application of the external magnetic field, so that when it is applied in the positive *z*-axis, the maximum Lorentz force acts on the inner winding of the small right coil and vice versa.

IV. Conclusion

The behavior of the QBC in a typical TMS operation and in a highly energized external field of 3T has been analyzed and computed. Under a typical TMS operating condition, the maximum magnetic flux density, Lorentz force density and von Mises stress were computed to be 5.7 T, 4.34 × 10^9 N/m^3 and 2.59 × 10^7 Pa respectively. With the application of an external field, the maximum values were observed in the *z*-axis of the QBC orientation and resulted in an increase of 39.65 %, 38.94 % and 94.59 % respectively from the typical TMS operation. With the increase however, the maximum

von Mises stress is still less than the yield strength of copper; 7.00×10^7 Pa. Therefore, we can conclude that the QBC will not deform under the effect of the external magnetic field. With the application of the external field in the *y*-axis of the QBC orientation, the magnitude of the parameters was greatly reduced by 12.28 %, 26.49 % and 22.78 % respectively. We can conclude also that the *y*-axis of the QBC orientation can be taken as an appropriate application axis during TMS-fMRI.

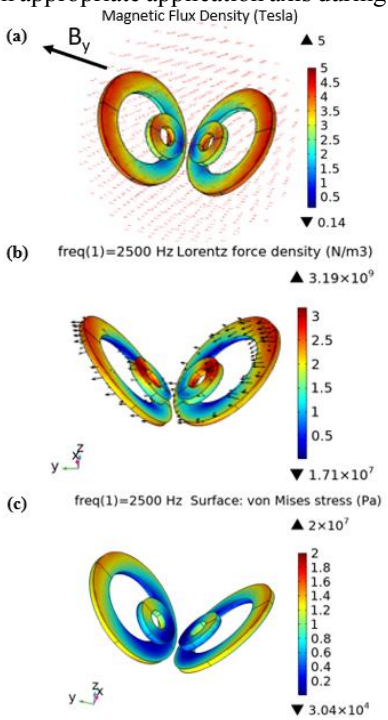

Fig. 4. (a) Magnetic flux density, $\boldsymbol{B}$ (T), (b) Resultant Lorentz force density, $\boldsymbol{f}$ (N/m^3), and (c) von Mises stress, σ_v (Pa) of the QBC in an energized magnetic environment applied parallel to the *y*-direction of the QBC.

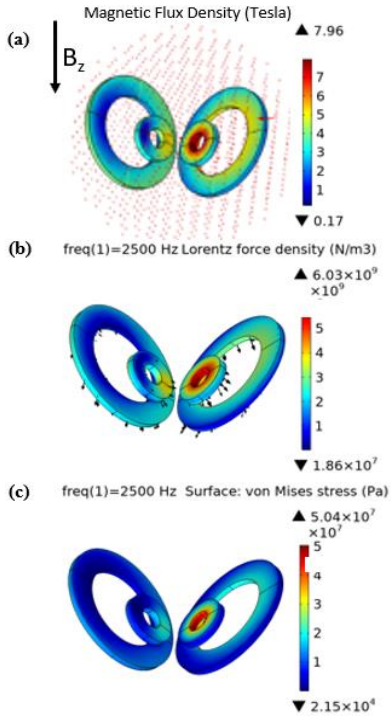

Fig. 5. (a) Magnetic flux density $\boldsymbol{B}$ (T), (b) Resultant Lorentz force density, $\boldsymbol{f}$ (N/m^3), and (c) von Mises stress, σ_v (Pa) of the QBC in an energized magnetic environment applied parallel to the *z*-direction of the QBC.

REFERENCES

[1] X. Zhong, P. Rastogi, Y. Wang, E. G. Lee, and D. C. Jiles, "Investigating the Role of Coil Designs and Anatomical Variations in Cerebellar TMS," *IEEE Transactions on Magnetics*, vol. 55, no. 7, pp. 1–5, Jul. 2019, doi: 10.1109/TMAG.2018.2890069.

[2] A. Chail, R. K. Saini, P. S. Bhat, K. Srivastava, and V. Chauhan, "Transcranial magnetic stimulation: A review of its evolution and current applications," *Ind Psychiatry J*, vol. 27, no. 2, pp. 172–180, 2018, doi: 10.4103/ipj.ipj_88_18.

[3] Shuo Yang *et al.*, "3D realistic head model simulation based on transcranial magnetic stimulation," in *2006 International Conference of the IEEE Engineering in Medicine and Biology Society*, Aug. 2006, vol. Supplement, pp. 6469–6472. doi: 10.1109/IEMBS.2006.260877.

[4] E. M. Wassermann and S. H. Lisanby, "Therapeutic application of repetitive transcranial magnetic stimulation: a review," *Clinical Neurophysiology*, vol. 112, no. 8, pp. 1367–1377, Aug. 2001, doi: 10.1016/S1388-2457(01)00585-5.

[5] Z.-D. Deng, S. H. Lisanby, and A. V. Peterchev, "Electric field depth–focality tradeoff in transcranial magnetic stimulation: Simulation comparison of 50 coil designs," *Brain Stimulation*, vol. 6, no. 1, pp. 1–13, Jan. 2013, doi: 10.1016/j.brs.2012.02.005.

[6] S. Ueno, T. Tashiro, and K. Harada, "Localized stimulation of neural tissues in the brain by means of a paired configuration of time-varying magnetic fields," *Journal of Applied Physics*, vol. 64, no. 10, pp. 5862–5864, Nov. 1988, doi: 10.1063/1.342181.

[7] P. Rastogi, E. G. Lee, R. L. Hadimani, and D. C. Jiles, "Transcranial Magnetic Stimulation: Development of a Novel Deep-Brain Triple-Halo Coil," *IEEE Magnetics Letters*, vol. 10, pp. 1–5, 2019, doi: 10.1109/LMAG.2019.2903993.

[8] Y. Roth, A. Zangen, and M. Hallett, "A Coil Design for Transcranial Magnetic Stimulation of Deep Brain Regions:," *Journal of Clinical Neurophysiology*, vol. 19, no. 4, pp. 361–370, Aug. 2002, doi: 10.1097/00004691-200208000-00008.

[9] P. Rastogi, E. G. Lee, R. L. Hadimani, and D. C. Jiles, "Transcranial Magnetic Stimulation-coil design with improved focality," *AIP Advances*, vol. 7, no. 5, p. 056705, May 2017, doi: 10.1063/1.4973604.

[10] M. J. Lan, B. T. Chhetry, C. Liston, J. J. Mann, and M. Dubin, "Transcranial Magnetic Stimulation of Left Dorsolateral Prefrontal Cortex Induces Brain Morphological Changes in Regions Associated with a Treatment Resistant Major Depressive Episode; an Exploratory Analysis," *Brain Stimul*, vol. 9, no. 4, pp. 577–583, 2016, doi: 10.1016/j.brs.2016.02.011.

[11] O. F. Afuwape, P. Rastogi, D. Jiles, and L. F. Ieee, "Effect of coil positioning and orientation of the quadruple butterfly coil during transcranial magnetic stimulation," *AIP Advances*, vol. 11, no. 1, p. 015212, Jan. 2021, doi: 10.1063/9.0000104.

[12] C. C. Ruff, J. Driver, and S. Bestmann, "Combining TMS and fMRI," *Cortex*, vol. 45, no. 9, pp. 1043–1049, Oct. 2009, doi: 10.1016/j.cortex.2008.10.012.

[13] P. Belardinelli *et al.*, "Reproducibility in TMS–EEG studies: A call for data sharing, standard procedures and effective experimental control," *Brain Stimulation*, vol. 12, no. 3, pp. 787–790, May 2019, doi: 10.1016/j.brs.2019.01.010.

[14] J. J. T. Vink, S. Mandija, P. I. Petrov, C. A. T. van den Berg, I. E. C. Sommer, and S. F. W. Neggers, "A novel concurrent TMS-fMRI method to reveal propagation patterns of prefrontal magnetic brain stimulation," *Hum Brain Mapp*, vol. 39, no. 11, pp. 4580–4592, Aug. 2018, doi: 10.1002/hbm.24307.

[15] L. Hernandez-Garcia, T. Hall, L. Gomez, and E. Michielssen, "A numerically optimized active shield for improved transcranial magnetic stimulation targeting," *Brain Stimulation*, vol. 3, no. 4, pp. 218–225, Oct. 2010, doi: 10.1016/j.brs.2010.05.001.

[16] L. J. Crowther, K. Porzig, R. L. Hadimani, H. Brauer, and D. C. Jiles, "Realistically Modeled Transcranial Magnetic Stimulation Coils for Lorentz Force and Stress Calculations During MRI," *IEEE Transactions on Magnetics*, vol. 49, no. 7, pp. 3426–3429, Jul. 2013, doi: 10.1109/TMAG.2013.2247578.